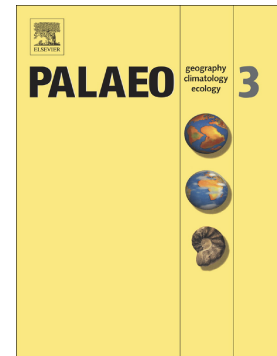# Accepted Manuscript

Nutrient influence on fossil carbonate factories: Evidence from SEDEX extractions on Burdigalian limestones (Miocene, NW Italy and S France)

Giovanni Coletti, Akram El Kateb, Daniela Basso, Alessandro Cavallo, Silvia Spezzaferri

Please cite this article as: Giovanni Coletti, Akram El Kateb, Daniela Basso, Alessandro Cavallo, Silvia Spezzaferri , Nutrient influence on fossil carbonate factories: Evidence from SEDEX extractions on Burdigalian limestones (Miocene, NW Italy and S France). The address for the corresponding author was captured as affiliation for all authors. Please check if appropriate. Palaeo(2017), doi: 10.1016/j.palaeo.2017.03.005

Nutrient influence on fossil carbonate factories: evidence from SEDEX extractions on Burdigalian limestones (Miocene, NW Italy and S France)

Giovanni Coletti[a]

Akram El Kateb[b]

Daniela Basso[c]

Alessandro Cavallo[c]

Silvia Spezzaferri[b]

a: corresponding author, g.coletti@campus.unimib.it; Department of Earth and Environmental Sciences of Milano-Bicocca University, Piazza della Scienza 4, 20126 Milano, Italy.

b: Department of Geosciences of Fribourg University, Chemin du Musée 6, 1700 Fribourg, Switzerland.c: Department of Earth and Environmental Sciences of Milano-Bicocca University, Piazza della Scienza 4, 20126 Milano, Italy.

Abstract

Different Miocene shallow-water carbonate successions have been examined to test the potential of phosphorus sequential extraction (SEDEX) in studying palaeo-nutrient levels, and to investigate nutrient influence on carbonate-factories during this epoch. The coralline-algal-dominated sequence of the Pietra da Cantoni Group (NW Italy) and the bryozoan-dominated sequence of the Sommières Basin (S France), have been targeted for this study. Actually, albeit they both developed during the Burdigalian, in the very same latitudinal zone, they present remarkably different carbonate factories. Palaeontological analyses have investigated the distribution of the major groups of carbonate-producing organisms throughout the successions. These results have been compared with those of geochemical analyses on phosphorus and organic matter abundance, testifying a clear relationship between the skeletal assemblage and the availability of nutrients. As

expected on the basis of modern oceanography and benthic ecology, bioavailable phosphorus concentration was higher in the bryozoan-dominated basin than in the coralline-algal-dominated basin. This result strongly supports SEDEX sequential extraction as a viable instrument to investigate the nutrient supply in the geological record. This also proves that the early-Miocene Mediterranean carbonate-factories were deeply controlled by nutrient influence, with patterns similar to those observed in present-day oceans. Moderate nutrient-concentrations resulted in coralline-algal dominance, while high nutrient-concentrations produced carbonate factories dominated by heterotrophs suspension-feeders like bryozoans. The euphotic-zone producers, which dominate in classical tropical associations, were probably restricted to areas with low nutrient-concentrations.

Key words

Phosphorus; bryozoans; large benthic foraminifera; hermatypic corals; Tertiary Piedmont Basin; Molasse Basin.

1. Introduction

Nutrient availability is a key factor for the distribution of carbonate-forming biota in modern oceans (Hallock, 1988, 2005; Hallock and Schalger, 1986; Carannante et al., 1988; Wood, 1993; Brasier, 1995a, b; Halfar et al., 2004; Wilson and Vecsei, 2005; Jessen et al., 2014). High nutrient-supply increases plankton biomass, providing more organic matter to heterotrophs, and reduces water-clarity due to the plankton and the organic particles suspended in the water column (Hallock, 1988, 2005; Brasier, 1995a;). Nutrification (*sensu* Hallock et al., 1993) may promote a shift from autotrophs-dominated, light-dependent association, toward a heterotrophs-dominated, light-independent association. Therefore, nutrient influence has been often used to justify the presence of heterozoan carbonates (*sensu* James, 1997), which commonly occur in cool climates, in an otherwise warm-water context (*e.g.* Carannante et al., 1988; Brandano and Corda, 2002;

Cunningham and Collins, 2002; Vannucci et al., 2003; Pomar et al., 2004; Reynaud and James, 2012; Coletti et al., 2015, 2016; Brandano et al., 2016). However, nutrient influence, in the vast majority of palaeoenvironmental reconstructions, is just assumed on the basis of fossil assemblages without direct measurement of the concentration of phosphorus, the ultimate limiting nutrient whose rate of supply regulates primary production over long timescales (Tyrrell, 1999). Most of techniques actually can measure only proxies related to phosphorus abundance (*e.g.* natural gamma radiation), or the total amount of phosphorus present in the rock (*e.g.* spectrophotometry). The latter are not direct expressions of bioavailable phosphorus since they consider also unaltered grains of detrital apatite, of igneous and metamorphic origins, which are not a bioavailable source of phosphate. Therefore, most of classical geochemical techniques may not be perfectly suitable to quantitatively study nutrient abundance in the fossil record.

The aim of this contribution is to use SEDEX sequential extraction, a methodology devised to separate and quantify bioavailable phosphorus from the total phosphorus (Ruttenberg, 1992; Slomp et al., 2002; Bodin et al., 2006; Ruttenberg et al., 2009), for the palaeoenvironmental reconstruction of two early Miocene carbonate successions: the Lower Unit of Sequence 2 (*sensu* Bicchi et al., 2006) of the Pietra da Cantoni Group of the Tertiary Piedmont Basin and the Sandy Molasse Unit of the Sommières Basin. This is a challenging goal using models of carbonate-factories distribution solely based on temperature and not taking into account trophic state. Actually, both sequences developed in climatic conditions that are expected to foster a classical warm-water association, but on the contrary their skeletal assemblages are largely dominated by temperate carbonate-producers. In this study the SEDEX extraction is combined with detailed palaeontological analyses to provide direct evidence, from separate and independent approaches, of nutrient influence on these Miocene carbonate-factories. This methodology will hopefully pave the way for a stronger integration of trophic state in the classification of carbonate facies.

2. Geological setting

The investigated carbonate successions were both located in the Northern part of the Mediterranean Basin (Fig. 1). During the Burdigalian the Pietra da Cantoni Group was less than 400 km east from the Sommières Basin and more or less at the same latitude (Dercourt et al., 2000). The region was roughly five degrees of latitude further south than today (Dercourt et al., 2000). Burdigalian climate in the area was warmer than present day (Adams et al., 1990; Billups and Scheiderich, 2010), with mean annual temperature above 20 °C even in Central Europe (Mosbrugger et al., 2005). The warm climate during the Burdigalian is also testified by the widespread occurrence of symbiont-bearing corals, whose area of distribution stretched all the way over the northern part of the Alpine Molasse Basin (Perrin and Bosellini, 2012).

The carbonate sequences of the Pietra da Cantoni Group (PDC from now onward) developed in the eastern Monferrato, a part of the Tertiary Piedmont Basin (NW Italy; Novaretti et al., 1995). During the Aquitanian, the deformation caused by the rotation of the Alpine Wedge uplifted and separated the Monferrato into an eastern and a western sector. The western sector was deep and dominated by a slope to basin environment, as testified by the deposition of diatom ooze (Bonci et al., 1990). The eastern sector was uplifted, resulting in the formation of an angular unconformity over which the PDC deposited, from Burdigalian to early Langhian (Clari et al., 1995; Novaretti et al., 1995). The PDC is divided into two different depositional sequences (Bicchi et al., 2006). The older sequence (Sequence 1, *sensu* Bicchi et al., 2006) is related to the first and localized marine transgression over the Eastern Monferrato area. The younger sequence (Sequence 2, *sensu* Bicchi et al., 2006) testifies the beginning of a transgressive trend in the area that will last for most of the Miocene. Rhodolith-rich, coarse skeletal-limestones dominate the Lower Unit of Sequence 2 (LU from now onward) while foraminiferal oozes dominate the Upper Unit (UU from now onward). A bed of condensed sediments, rich in glaucony and phosphates, separates the two units (Schüttenhelm, 1976; Bicchi et al., 2006). This interval testifies a period of major sediment starvation, caused by the drowning of the carbonate factory and is included, from the environmental point of view, in the UU, which is dominated by the activity of the pelagic carbonate factory

(Coletti et al., 2015). The rhodalgal (*sensu* Carannante et al., 1988) carbonates of the LU are investigated in this study, their deposition should have occurred in the Burdigalian, between 19 and 18 Ma (Novaretti et al., 1995; Ruffini, 1995; D'Atri et al., 1999, 2001; Coletti et al., 2015; Fig. 2).

During the early Burdigalian the sea flooded the Alpine Molasse Basin, creating a narrow, tide-dominated, seaway connecting the western Mediterranean with the Parathetys Basin (Allen et al., 1985; Dercourt et al., 2000; Reynaud and James, 2012). In southeastern France, at the junction between the Molasse sea and the Mediterranean, the marine transgression lead to the deposition of extensive, tide-controlled, shelf deposits over the folded Mesozoic and Paleogene strata (Besson et al., 2005; Reynaud et al., 2006; Reynaud and James, 2012). The Sommières Basin was a small embayment, connected to the Alpine Molasse Basin through a flooded valley (Reynaud and James, 2012). Within the Sommières Basin two different depositional sequences are recognized, which include three units: the Sandy Molasse, the Sandy Marls and the Calcareous Molasse (Demarcq, 1970; Reynaud and James, 2012; Fig. 2). The first sequence includes the Sandy Molasse and the Sandy Marls, while the second sequence corresponds to the Calcareous Molasse (Reynaud and James, 2012). The Sandy Molasse Unit (SMU from here onward), which is analyzed in this study, is characterized by coarse-grained, bryozoans-dominated, heterozoan carbonates and it represents the transgressive tract of the first sequence (Reynaud and James, 2012). Microbioclastic wakestones and mudstones dominate the overlaying Sandy Marls Unit, which represents the high stand of the first sequence (Reynaud and James, 2012; Fig. 2). The end of the deposition of the Sandy Marls Unit is followed by an abrupt sea level fall (Reynaud and James, 2012). The overlaying Calcareous Molasse Unit represents the second marine transgression (Reynaud and James, 2012). A marly interbed of the Calcareous Molasse Unit suggests a middle late-Burdigalian age for this unit (zone M4, *sensu* Berggren et al., 1995; 17.5 to 16.4 Ma, Wade et al., 2011), thus supporting an early Burdigalian age for the SMU (Berger, 1974; Reynaud and James, 2012; Fig. 2).

3. Material and Methods

In order to have samples with as little alteration as possible, the material was collected on fresh surfaces inside the quarries of Uviglie (LU), Pondres and Souvignargues (SMU; Fig. 1). Moreover, the samples were taken after the removal of the most superficial part of the rock that might have been weathered. On the basis of rock texture and macroscopic fossiliferous content, a number of homogeneous lithozones (numbered from the oldest to the youngest) were identified in each outcrop and very large (>2 kg), representative, samples were collected from each lithozone. A total of eighteen samples was collected from the two succession, one from each lithozone, except than in Souvignargues succession were more samples were collected to further assess the uniformity of the material (the results from Souvignargues samples were averaged during the elaboration). Serving as internal reference point of low phosphorus concentration, a sample of coral-reef limestone of late Miocene age (Fig. 1; Balza di Rocca Limata, Terravecchia Formation, Sicily, Grasso and Pedley, 1988) was also included in the SEDEX analysis. This material was chosen because it was a perfect, *in situ*, fossil counterpart of present-day reefs which are oligotrophic environments. Actually, reefs truly comparable to those of modern tropical oceans, arose in the Mediterranean only in the late Miocene (Pomar and Hallock, 2007, 2008).

The SEDEX sequential extraction allows an accurate quantification of the different P-minerals of a sample. These are: exchangeable (or loosely-bound) P, Fe-oxyhydroxides-bound P, authigenic and biogenic Ca-P minerals, organic P and detrital apatite (Ruttenberg, 2004). Except detrital apatite, all these minerals are sinks for the reactive P present in the water (Ruttenberg, 1992); therefore, the sum of their contribution to the total phosphorus pool has been used in this study as a proxy for nutrient availability in the palaeoenvironment (bioavailable phosphorus). The extraction was performed according to Ruttenberg et al. (2009), which proposed an improved version of the original SEDEX sequential extraction (Ruttenberg, 1992) aimed to reduce procedural flaws and losses of material. From each sample approximatively 15 g of rock fragments (randomly picked from the large sample to obtain a representative result) were pestled in an agate mortar and homogenized completely in order to pass through a 125 μm mesh sieve (Ruttenberg et al., 2009).

For each sample, 80 mg of the sieved material were analyzed in the sequential extraction at the University of Fribourg Switzerland (Stalder et al., 2014). The remaining of the grounded samples was used for quantitative X-ray powder diffraction, total organic carbon (TOC) analysis and C/H/N elemental analysis.

C/H/N and TOC analyses were performed at the laboratory of Sediment Geochemistry at the University of Lausanne (Switzerland) on about 100 mg of bulk grounded sediment using the Rock-Eval6 technology and following the standard rock pyrolysis procedure (Espitalié et al., 1985; Behar et al., 2001); a portion of each sample was stored as archive. In cases of TOC <0.1 % further interpretation on the origin of the organic matter, using pyrolysis parameters and elemental composition, were considered unreliable due to both the low TOC and the high rock-matrix effect of limestone (Katz, 1983; Langford and Blanc-Valleron, 1990; Nuñez-Betelu and Baceta, 1994).

X-ray powder diffraction (XRPD) analysis was performed at the Milano-Bicocca laboratories using a Bragg–Brentano θ-θ PANalytical X'Pert PRO PW3040/60 X-ray powder diffractometer. The limit of detection of XRPD depends on the mineral phase (cristallinity, structural disorder), and is generally comprised between 0.1 wt% (for highly crystalline phases) and 5 wt%. The qualitative phase analysis was performed using the PANalytical HighScore Plus software version 2.2c; quantitative phase analysis was carried out using the Rietveld method (Rietveld, 1969), following the refinement strategies described in Gualtieri (2000). Refinements were accomplished with the GSAS package (Larson and Von Dreele, 1999) and its graphical interface EXPGUI (Toby, 2001).

To further study authigenic minerals, scanning electron microscope observations (SEM) and energy-dispersive X-ray spectroscopy (EDS) analyses were performed on carbon-coated thin sections (at Milano-Bicocca laboratories, with a Tescan VEGA TS Univac 5136 XM Scanning Electron Miscroscope coupled with an EDAX Genesis 4000 XMS Imaging 60 SEM Energy Dispersive Spectrometer).

Petrographic characteristics and skeletal assemblages of the limestones were studied with point-counting technique performed on digital photomicrographs of thin sections (Flügel, 2010). For each sample more than 400 points were identified. Coralline-algal distribution was further investigated in thin sections, by measuring, with a vector graphics editor (Inkscape release 0.91 for Ubuntu), the area covered by the different taxa of coralline algae. Coralline suprageneric identification follows Le Gall et al. (2009), Nelson et al. (2015), Rösler et al. (2016).

4. Results

4.1 Skeletal assemblage

4.1.1 Uviglie

The Uviglie succession includes seven lithozones and encompasses both the LU and the UU (Fig. 3A, B). The LU is at the base of the succession and includes lithozones UV1-UV4a, which are composed of coarse-grained skeletal elements produced by a benthic carbonate-factory (Table 1; Figs 3-4). The bioclasts are often fragmented and abraded. Extensive evidences of dissolution (e.g. moldic porosity) were not observed. Coralline algae largely dominates the skeletal assemblage (Table 1; Fig. 3A, C, D; Fig. 4). Coralline fragments are extremely abundant in the <2 mm fraction in all the LU, while whole rhodoliths are common in UV1 and UV3 and extremely common in UV2, UV4a and UV4b (Table 1; Fig. 3A; Fig. 4). Coralline-algal assemblage is largely dominated by Hapalidiales, while Sporolithales and Corallinales contribution is minimal (Table 1; Fig. 3C, D). Barnacles are also very frequent, especially in UV3, UV4 and UV4b (Table 1; Fig. 3D, E; Fig. 4). Benthic foraminifera and in particular large benthic foraminifera (*Nephrolepidina*, *Eulepidina*, *Miogypsina*, *Amphistegina* and *Operculina*) are common, especially in UV1 (Table 1; Fig. 3F; Fig. 4). Mollusks, echinoids and bryozoans are minor components, while ostracods and serpulids are rare (Table 1).

The UU is mainly composed of planktonic elements and occurs in the upper part of the succession. Planktonic foraminifera are common in lithozones UV4b, become extremely abundant

in lithozone UV5 and overwhelmingly dominates the skeletal assemblage in lithozone UV6 (Table 1). Conversely, benthic skeletal elements, highly abraded and often phosphatized and glauconized, are common in UV4b and UV5, while they are almost absent in UV6 (Table 1).

4.1.2 Souvignargues and Pondres

The SMU includes lithozones SOUV1 and PON1-PON5 (Figs 4, 5). The rock is coarse-grained and mainly composed of bioclasts of benthic origin (Table 1; Figs 4-5), which are often highly abraded and fragmented, especially in SOUV1, where the grains are also well rounded. Extensive evidences of bioclasts dissolution and conspicuous moldic-porosity were not observed. Bryozoans dominate the skeletal assemblage (except in lithozone PON3, where coralline algae are more abundant; Table 1; Fig. 4; Fig. 5A, B). They are extremely common in the <2 mm fraction and gravel-sized bryozoans-nodules occur in lithozones SOUV1, PON1 and PON5 (Fig. 5A). Encrusting bryozoans commonly occur within rhodoliths. Coralline algae are also very frequent in the <2 mm fraction and they occur in >2 mm fraction as rhodoliths (rare) and unattached branches (Table 1; Figs 4; Fig. 5C, D). The coralline association of the SMU is largely dominated by Hapalidiales (Table 1; Fig. 5D, E). Corallinales and Sporilthales are far less common (Table 1). Mollusks and echinoids are very common, while barnacles are uncommon (Table 1; Fig. 4). Benthic foraminifera are rare, especially large benthic foraminifera (LBF from here onward), among them the only recognized genus is *Amphistegina* (Table 1; Fig. 4; Fig. 5F). Brachiopods, ostracods and serpulids are very rare (Table 1).

4.1.3 Coral-reef limestone of Balza di Rocca Limata

The Messinian coral-reef limestone of Balza di Rocca Limata (Central Sicily, Southern Italy) belongs to the Terravecchia Formation (Grasso and Pedley, 1988). It consists of a large (45m high and 2km wide), *in situ*, coral reef formed by branched colonies of *Tarbellastrea* and scattered

colonies of *Porites*, both massive and branched. The skeletal assemblage of the unit is almost entirely composed of hermatypic corals (Table 1).

4.2 Phosphorus content, petrography, mineralogical composition and organic matter content

4.2.1 Uviglie

The LU and the UU are clearly separated from the mineralogical point of view (Table 1; Fig. 4). Lithozones UV1-UV4a, dominated by benthic carbonate production, are mainly composed of carbonate minerals (Table 1; Fig. 4). On the other hand, silicate minerals are much more abundant in the lithozones UV5 and UV6, which are dominated by planktonic carbonate production (Table 1; Fig. 4). Lithozone UV4b, has an intermediate composition (Table 1; Fig. 4). This difference in mineralogical composition, resulting from XRPD analyses, is also supported by point counting observations that show an increase in the detrital fraction and in the abundance of authigenic minerals (Table 1; Fig. 6A, B). In lithozones UV1-UV4a glaucony grains are rare, small and pale green in color, while in lithozones UV4b-UV6 they are far more common, larger and of a deep-green color (Fig. 6A).

The concentrations of both detrital phosphorus and bioavailable phosphorus are far higher in lithozones UV4b-UV6 than in lithozones UV1-UV4a (Table 1; Fig. 4). The average bioavailable P content of the latter group is 24.9 µmol/g of sediment, detrital P contribution is 0.6 µmol/g (Table 1; Fig. 4). The former group have an average concentration of 91.4 µmol/g of bioavailable P and of 64.9 µmol/g of detrital P (Table 1; Fig. 4). This difference is also supported by XRPD that shows the abundant presence of Carbonate-Apatite in lithozones UV5 and UV6 (Table 1)

The TOC of the samples is always <0.1 %. The low content in organic matter is also testified by the low amount of organic phosphorus resulting from SEDEX extractions. Organic P represents around 1 % of the bioavailable P and only in the samples of the UU it represents around 10% of the bioavailable P.

4.2.2 Souvignargues and Pondres.

In all the lithozones silicate minerals are quite abundant. This is supported by both XRPD analyses and point-counting (Table 1; Fig. 4). It must be stressed that, in this instance, the detrital fraction is underestimated by XRPD analyses. This technique cannot separate the carbonate of the skeletal grains from the limestone rock-fragments, eroded from the Cretaceous-Oligocene bedrock of the basin. The latter are very common, especially in the succession of Souvignargues (lithozone SOUV1). Actually, according to point-counting, the detrital fraction represents, on average, between 25% to 30% of the whole rock (Table 1; Fig. 4).

In all the samples, small amounts of authigenic minerals are present, both phosphates and glaucony grains with a very low degree of maturity (Fig. 6C-H).

The phosphorus distribution is quite uniform in the SMU. The average concentration of bioavailable P of the two succession is 40.6 µmol/g, the highest values are recorded in SOUV1 and the lowest in PON3 (Table 1; Figs 4, 5). The average concentration of detrital P is 2.3 µmol/g and only minor differences occur between the different lithozones (Table 1; Fig. 4).

The TOC is <0.1 % in all samples. The low content in organic matter is also testified by the low amount of organic phosphorus resulting from SEDEX extractions (≈1 % of bioavailable P).

4.2.3 Coral-reef limestone of Balza di Rocca Limata.

The coral-reef limestone is almost entirely composed of carbonate minerals. It has a bioavailable P concentration of 16.8 µmol/g and a detrital P concentration of 0.9 µmol/g (Table 1). This limestone is also characterized by a very low content in both organic matter and organic phosphorus.

5. Discussion

5.1 Skeletal assemblages

The two early-Miocene successions present skeletal-assemblages that are regarded as characteristic of temperate water (Lees and Buller, 1972). Actually, they are dominated by bryozoans, coralline algae, barnacles and benthic foraminifera (Table. 1; Fig. 4). On the other hand, evidences of tropical climate can be found in both successions. LBF occur in the LU and in the SMU, diverse and common in the former and rare in the latter. LBF suggest warm water with temperature above 14 °C throughout the year and yearly average temperature above 20 °C (Beltzer et al., 1997; Geel, 2000; Langer and Hottinger, 2000; Beavington-Penney and Racey, 2004). Among coralline algae, *Sporolithon* and *Lithoporella*, which are both tropical genera (Adey, 1979; Fravega et al., 1989; Vannucci et al., 1996), occur in both areas. General palaeoclimatic reconstructions suggest warm climate during the early Miocene and the persistence of tropical conditions in the Mediterranean region during the Burdigalian (Zachos et al., 2001; Pomar et al., 2004; Mosbrugger et al., 2005). A northward expansion of symbiont-bearing corals is recorded in the circum-Mediterranean realm during this stage, with small patches of corals (*e.g. Tarbellastrea*; Kühn, 1963) even in the Northern Alpine Molasse Basin, hundreds of kilometers further north than the two localities investigated in this study (Perrin and Bosellini, 2012). It must be stressed that hermatypic corals before the late Miocene, although always restricted to tropical settings, were probably different from their modern counterparts. They did not build reefs up to the sea-level but rather produced mounds in the middle shelf, leaving the upper photic-zone to seagrasses and green calcareous algae (Brandano, 2003; Pomar and Hallock, 2007; Brandano et al., 2015). Nevertheless, Burdigalian corals probably still required more light than coralline algae and LBF, since coral facies is usually found shoreward than the facies dominated by coralline algae and LBF (Civitelli and Brandano, 2005; Brandano et al., 2007, 2010; Benisek et al., 2009).

Since the climate in the area was tropical, environmental factors other than temperature caused the absence of the typical tropical-facies in the studied successions. Nutrient supply strongly affects carbonate-producing organisms (Hallock and Schalger, 1986; Wood, 1993; Mutti and Hallock, 2003). In modern oceans a shift from symbiont-bearing corals to coralline-algal-

dominated environment can occur in response to a modest increase in nutrient flux, while a shift

from corals to a heterotroph-dominated biota can result from a substantial increase in nutrient flux

(Hallock, 2001). At tropical latitudes, in the Gulf of California, consistently with a strong gradient

in nutrient concentration, different carbonate factories exist: coral reefs dominate where nutrient

supply is low, coralline algae where the supply is moderate, and bryozoans and mollusks where the

supply is high (Halfar et al., 2004, 2006, 2012). In the Atlantic Ocean the Northern Mauritania

shelf hosts an heterotrophs-dominated association thanks to upwelling currents (Klicpera et al.,

2013). The same effects can be observed at the Equator in the Galapagos Archipelago where, due to

upwelling currents, carbonate production is dominated by heterotrophs (Reymond et al., 2016). At

similar latitudes, a shift from euphotic to oligophotic carbonate producers occurs in the Spermonde

Shelf (Sulawesi, Indonesia). The shelf is mesotrophic due to river run-off and carbonate production

is dominated by LBF, while corals are restricted to areas protected from terrestrial influence

(Renema and Troelstra, 2001; Wilson and Vecsei, 2005). LBF cope better than corals in nutrient-

rich environments, but they exhibit greater species diversity in stable oligotrophic conditions

(Hallock and Schalger, 1986; Renema and Troelstra, 2001; Beavigton-Penney and Racey, 2004). In

situ nutrient-enrichment experiments further suggest that corals settlement is negatively impacted

by an increase in nutrient supply (Jessen et al., 2014). Bryozoans recruitment, on the other hand, is

increased (Jessen et al., 2014). Recruitment experiments along the eastern coasts of Australia, also

confirmed that coralline algae and corals are more abundant far away from terrestrial run-off, while

bryozoans (especially encrusting cheilostomatids) are more common near shore in, nutrient rich,

turbid water (Holmes et al., 1997).

Nutrient influence has already been recognized as an important element in the

reconstruction of fossil carbonate factories (*e.g.* Carannante et al., 1988; Brasier, 1995b; Brandano

and Corda, 2002; Cunningham and Collins, 2002; Hageman et al., 2003; Vannucci et al., 2003;

Pomar et al., 2004; Reynaud and James, 2012; Brandano et al., 2016). Therefore, we suggest that

nutrient supply-rate had a major impact on the investigated early-Miocene systems, driving out

hermatypic corals and euphotic algae, and fostering the dominance of heterotroph suspension-feeders (bryozoans and barnacles) and oligophotic autotrophs and mixotrophs (coralline algae and LBF). The former were favored by plankton abundance and the latter by the lack of competitors due to the turbid water. Hapalidiales, which thrive in low-light conditions (Aguirre et al., 2000), dominate coralline assemblages in both localities, even in very shallow settings associated with barnacles (UV3-UV4a; Table 1), and in proximity of the shoreline (SOUV1; Table 1; Fig. 2), thus supporting the presence of turbid water.

Nutrient supply-rate can also explain the differences between the two studied systems. During the Burdigalian, the two basins were at the same latitude and they were separated just by a few hundreds of kilometers, therefore, significant climatic differences are unlikely (Fig. 1). Furthermore, the texture of the material suggests that both skeletal assemblages developed in a relatively shallow-water setting, thus excluding major variations related to water depth. The coralline-barnacle-LBF association of the LU probably developed under moderate nutrient-supply, while high nutrient-supply and really turbid-water fit perfectly with the bryozoans dominance of the SMU (Fig. 4).

It should be pointed out that skeletal assemblages result from a suite of environmental controls that also includes sedimentary processes like sediment transport and reworking. In both sequences there is evidence of sediment transport (Reynaud and James, 2012; Coletti et al., 2015). However, in both successions, the same skeletal assemblage is recognized within the rhodoliths (trapped and protected between the algal crusts, *sensu* Coletti et al., 2015), and in the host lithology, suggesting a negligible influence of reworking and transport processes over the final composition of the fossil associations. Selective loss of aragonite is another possible source of distortion, but the lack of conspicuous moldic-porosity suggests that the associations were not severely affected by dissolution. Finally, although secondary processes might have slightly influenced the skeletal assemblages, the observed differences between the contributions of the major carbonate-producers are so large (*e.g.* bryozoans are ten times more abundant in the SMU

than in the LU; Table 1; Fig. 4), that they could have only be caused by environmental factors, namely nutrient concentration.

5.2 Phosphorus concentration

The concentrations of bioavailable P, measured with SEDEX extractions, support the supply-rates of nutrients reconstructed on the basis of the benthic skeletal-assemblages. The average concentration of bioavailable P in the SMU is higher than in the LU (lithozones UV1-UV4a). Bioavailable P concentrations of both localities are higher than the bioavailable P concentration in the coral-reef limestone of Balza di Rocca Limata, which was supposed to have the lowest concentration of P in the data set, since coral-reefs are oligotrophic environments (Table 1; Fig. 4).

The highest values of bioavailable-P are recorded in the UU, in agreement with XRPD analyses that indicate abundant authigenic phosphates in these samples (Table 1; Fig. 4). It must be considered that the abundance of authigenic minerals is also related to the sedimentation rate, and large concentrations of these minerals develop when the rate is low (Föllmi, 2016). Lithozones UV4b-UV6 deposited during a period of sediment starvation, as evidenced by the abundance and the characteristics of glaucony (Table 1; Fig. 6A, B). Actually, glaucony grains occur throughout the whole Uviglie succession, but in the LU they are uncommon and their characteristics suggest a low degree of maturity (*sensu* Amorosi, 1995, 1997), while in the UU they are abundant and they have an high degree of maturity (Fig. 6A). Therefore, the sharp increase in bioavailable P between the LU and the UU of PDC, is mainly related to a drop in sediment accumulation-rate caused by the drowning of the carbonate factory due to sea-level rise (Coletti et al., 2015). Lithozone UV4b, which testifies the inception of sediment starvation after the drowning of the carbonate factory (Coletti et al., 2015), has an intermediate composition. Rare grains of glaucony with a very-low degree of maturity occur in the SMU (Fig. 6D), suggesting a sedimentation rate higher than the one of the LU, where more mature glaucony occurs. Therefore, if a correction was included to account

for the difference in sedimentation rate, this would have been in favor of the SMU, thus widening the gap between the results from the two basins.

The recorded concentrations of bioavailable P could have been influenced also by the post depositional and diagenetic histories of the two units. Under anoxic conditions, the P adsorbed on Fe-oxyhydroxides surfaces is released back in to the water column (Krom and Berner, 1981). However, there are no palaeoecological evidences suggesting anoxia in the palaeoenvironment. Oxic conditions, supporting the rapid decomposition of organic matter at the seafloor, are also testified by the low concentrations of TOC. Authigenic Ca-P minerals (Carbonate-fluorapatite) are another major sink of bioavailable P (Ruttenberg and Berner, 1993). These minerals are more resistant to alteration than carbonate minerals (calcite, magnesite and dolomite) and display the same dissolution rate of albite (Guidry and Mackenzie, 2003). Furthermore, P is preferentially retained in the crystal lattice during the early stages of the dissolution process (Guidry and Mackenzie, 2003). Only in acid conditions occurring in soils, these minerals dissolve completely and lose their P (Guidry and Mackenzie, 2003). The low amount of organic matter present in the studied samples, suggests that they were not affected by soil and plant-related alteration processes (Ma et al., 2007; Marinoni et al., 2007; Jaquat et al., 2009; Cabadas et al., 2010). The overall diagenetic history of the two units is very similar: very shallow burial, very limited tectonic deformation and meteoric diagenesis. Their texture and porosities are also similar. Therefore, if any diagenetic alteration occurred, the process should have modified the original composition in the same way in both localities, thus preserving the original nutrient signal.

Taking into account all these evidences, the hypothesis that the measured concentrations of bioavailable P are just the random results of depositional and diagenetic processes is unlikely. On the contrary, these values reflect original differences in nutrient supply-rates which are also faithfully recorded by the skeletal-assemblages of the benthic carbonate factories.

5.3 Palaeoenvironmental reconstruction

The PDC carbonate system developed on an isolated bank uplifted by the rotation of the Alpine Wedge (Maffione et al., 2008) and therefore protected from the siliciclastic detritus eroded from the Alps (Fig. 7A). The presence of rare angular rock-fragments, eroded from older formations (Coletti et al., 2015), suggests that small and low-lying emerged lands existed at the time. These small islands however were clearly not a large source of detritus and nutrients. Actually, the LU is composed only of pure limestone with minimal siliciclastic contribution (Table 1; Fig. 4). Accordingly, also the detrital-P fraction of the total P is minimal (Table 1; Fig. 4). Only during the deposition of the UU, after the drowning of the carbonate platform, the detrital fraction became more important (Table 1; Fig. 4). The bioclastic contribution of the benthic carbonate factory had been reduced to almost zero and, without the protection of the now-submerged islands, the PDC basin was more exposed to fluxes of alpine detritus. Within this setting, it is unlikely that nutrients were supplied to the LU carbonate factory by river runoff. An upwelling source is more consistent with the very low concentration of detrital P in the LU (Fig. 7A). The deposition of siliceous ooze westward from PDC area (Bonci et al., 1990) also supports this hypothesis. The upwelling provided the PDC basin with a moderate supply of nutrients, resulting in turbid water that supported oligophotic production even in shallow settings, as testified by Hapalidiales associated with barnacles and coarse-grained sediments. The resulting carbonate factory was dominated by coralline algae, with important contribution of barnacles and LBF (Fig. 7A).

The Sommières Basin was almost completely enclosed by land (Reynaud and James, 2012; Fig. 7B) and the contribution of the detrital fraction was remarkably more important (Table 1; Fig. 4). Detrital-P concentrations are also higher than in the LU and there is a direct correlation between the siliciclastic fraction and the total-P concentration (Table 1; Fig. 4). Actually, the near-shore succession of Souvignargues has a higher P concentration than the more off-shore succession of Pondres (Table 1; Fig. 4). Therefore, it is likely than in the Sommières Basin the source of nutrients was land based, either due to small rivers or directly from the runoff of the land (Fig. 7B). These

sources provided the strong injection of nutrients that fostered bryozoans dominance in the basin (Fig. 7B). Water clarity was significantly reduced, favoring the aphotic production of heterotrophs suspension-feeders even in proximity of the shoreline. LBF were negatively affected by these conditions and only stress-resistant taxa were able to survive (Fig. 7B). Coralline algae, which can live even with very-low levels of light, were still abundant, but less common than in the the PDC system (Fig. 7).The distribution of these Miocene carbonate factories along a nutrient gradient is remarkably similar with the one observed at tropical latitude in the Gulf of California, where hermatypic corals, coralline algae, and bryozoan-dominated assemblages follow one another along a strong gradient of increasing nutrient concentrations (Fig. 7C; Halfar et al., 2004, 2006). During the early Miocene, the general pattern of distribution of Mediterranean carbonate-factories along a nutrient gradient was probably also comparable to the modern one. Low-nutrient settings were dominated in shallow water by euphotic producers (seagrasses and green calcareous algae), while in the middle platform the contribution of mesophotic hermatypic-corals was important. Systems with intermediate nutrient-supply were generally dominated by oligophotic producers (coralline algae and LBF). Under high nutrient-concentration the production was dominated by the aphotic production of heterotroph suspension-feeders (bryozoans, barnacles, mollusks; Fig. 7D). It must be stressed that, without an accurate assessment of nutrient levels, these pattern of distribution could be easily mistaken for variations along a temperature gradient. Since trophic state is just as important as temperature in controlling carbonate factories, palaeoenvironmental reconstruction based on skeletal-assemblages, should evaluate both factors to produce reliable interpretations.

6. Conclusions

The carbonate factories of the Lower Unit of Pietra da Cantoni Group (LU of PDC, Tertiary Piedmont Basin) and of the Sandy Molasse Unit (SMU, Sommières Basin), developed in the Northern Mediterranean region during a period of warm climate of the Burdigalian. However, temperate skeletal assemblages characterized these successions. Actually, due to the abundant

nutrient supply, most of tropical, oligotrophic, carbonate-producers were driven out from the association. Coralline algae were able to thrive in these turbid water and heterotrophs suspension-feeders flourished thanks to the plentiful supply of particulate organic carbon.

In the Pietra da Cantoni Group, moderate nutrient concentrations fostered the development of a coralline-dominated carbonate factory, with important contribution of large benthic-foraminifera and barnacles. Nutrients were supplied to this isolated bank by the upwelling of deep water from the western sectors of the Tertiary Piedmont Basin.

The Sommières Basin was located at the same latitude of the Tertiary Piedmont Basin, a few hundreds of kilometers westward, on the other side of the rising Alpine mountain range. The basin was almost land-locked with only a narrow seaway connecting the inlet with the Alpine Molasse Basin. Small rivers and/or direct terrestrial runoff provided a strong injection of nutrients. The resulting high-nutrient concentrations fostered a bryozoan-dominated carbonate factory with important contribution of coralline algae. The high nutrient concentrations were detrimental to large benthic-foraminifera and only stress-resistant taxa were able to survive.

Palaeontological evidences are in agreement with the results of SEDEX analyses on P content. The latter indicates remarkably higher abundance of bioavailable P in the bryozoan-dominated association of the Sandy Molasse Unit of Sommières Basin than in the coralline-algal-dominated association of the Lower Unit of Pietra da Cantoni Group. The concentrations of bioavailable P in both successions are higher than those of a Miocene coral-reef limestone. These results strongly suggest that SEDEX sequential extraction is a viable instrument to investigate palaeo-nutrient levels in shallow-water carbonates, opening new research possibilities in the field of palaeoenvironmental reconstructions.

Acknowledgments

References

Acker J.G., Leptoukh G. (2007) – Online analysis enhances use of NASA Earth Science data. Eos Transactions American Geophysical Union, 88, 14-17.

Adey W.H. (1979) – Crustose coralline algae as microenvironmental indicators in the Tertiary. In Gray J., Boucout A.J. (eds.): Historical Biogeography, Plate Tectonics and the changing Environment, 459-464.

Adams C.G., Lee D.E., Rosen R.B. (1990) – Conflicting isotopic and biotic evidences for tropical sea-surface temperatures during the Tertiary. Palaeogeography Palaeoclimatology Palaeoecology, 77, 289-313.

Aguirre J., Riding R., Braga J.C. (2000) – Late Cretaceous incident light reduction: evidence from benthic algae. Lethaia, 33, 205-213.

Allen P., Mange-Rajetzky M., Matter A., Homewood P. (1985) – Dynamic paleogeography of the open Burdigalian seaway. Swiss Molasse Basin. Eclogae Geologicae Helveticae, 78, 351-381.

Amorosi A. (1995) - Glaucony and sequence stratigraphy: a

conceptual framework of distribution in siliciclastic sequences. Journal of Sedimentary

Research, 65, 419-425.

Amorosi A. (1997) - Detecting compositional, spatial and temporal attributes of glaucony: a tool

for provenance research. Sedimentary Geology, 109, 135-153.

Beavington-Penney S.J., Racey A. (2004) – Ecology of extant nummulitids and other large

benthic foraminifera in paleoenvironmental analysis. Earth-Science Reviews, 67, 219-265.

Behar F., Beaumont V., Penteado H.I.DeB. (2001) – Rock-Eval6 technology: performances and

developments. Oil & Gas Science and Technology, 56, 111-134.

Beltzer C., Brachert T.C., Nebelsick J. (1997) – The warm temperate carbonate province: a

review of the facies, zonations and delimitations. Courier Forschungsinstitut Senkenberg, 201,

83-99.

Berger G.M. (1974) – Carte gèologique de la France à 1/50000. Sommières (n°964), BRGM,

Orlèans.

Berggren W.A., Kent D.V., Swisher C.C., Aubry M.P. (1995) – A revised cenozoic

geocrhonology and chronostratigraphy. In: Berggren W.A., Kent D.V., Aubry M.P., Hardenbol J.

(eds.) - Geochronology, Time Scale and Global Correlations: An Unified Temporal

Frame-work for Historical Geology. SEPM Special Publication, 54, 129–212.

Besson D., Parize O., Rubino J.L., Aguilar J.P., Aubry M.P., Beaudoin B., Berggren W.A., Clauzon G., Crumeyrolle P., Dexcoté Y., Fiet N., Iaccarino S., Jiménez-Moreno G., Laporte-Galaa C., Michaux J., Salis K., Suc J.P., Reynaud J.Y., Wernli R. (2005) – Un réseau fluviatile d'âge Burdigalien terminal dans le Sud-Est de la France : remplissage, extension, âge, implications. Comptes Rendus Geoscience, 337, 1045-1054.

Bicchi E., Dela Pierre F., Ferrero E., Maia F., Negri A., Pirini-Radrizzani C., Radrizzani S., Valleri G. (2006) – Evolution of the Miocene carbonate shelf of Monferrato (North-western Italy). Bollettino della Società Paleontologica Italiana, 45, 1-24.

Billups K., Scheiderich K. (2010) – A synthesis of Oligocene trough Miocene deep sea temperatures as inferred by Mg/Ca ratios. In: Mutti M., Piller W.E., Betzler C. (eds.) - Carbonate system during the Oligocene-Miocene Climatic Transition. International Association of Sedimentologist, Special Publication, 42, 1-16.

Bodin S., Godet A., Föllmi K.B., Vermeulen J., Arnaud H., Strasser A., Fiet N., Adatte T. (2006) – The late Hauterivian Faraoni oceanic anoxic event in the western Thethys: Evidence from Phosphorus burial rates. Palaeogeography Palaeoclimatology Palaeoecology, 235, 245-264.

Bonci C., Clari P.A., Ferrero E., Ghiribaudo G., Pirini C., Ricci B., Valleri G., Violanti D. (1990) – Diatomites of Marmorito (Western Monferrato, Norhtern Italy). Memorie di Scienze Geologiche dell'Università di Padova, 42, 189-225.

Brandano M., Corda L. (2002) – Nutrients, sea level and tectonics: constrains for the facies architecture of a Miocene carbonate ramp in central Italy. Terra Nova, 14, 257–262.

Brandano M. (2003) – Tropical/subtropical inner ramp facies in lower Miocene "Calcari a Briozoi e Litotamni" of the Monte Lungo Area (Cassino Plain, Central Apennines, Italy). Bollettino della Società Geologica Italiana, 122, 85-98.

Brandano M., Vannucci G., Mateau-Vicens G. (2007) – Le alghe rosse calcaree come indicatori paleoambientali: l'esempio della rampa carbonatica Laziale-Abruzzese (Burdigaliano, Appennino centrale). Bollettino della Società Geologica Italiana, 126, 55-69.

Brandano M. Tomasetti L., Bosellini F., Mazzucchi A. (2010) – Depositional model and paleodepth reconstruction of coral-rich mixed siliciclastic-carbonate system: the Burdigalian of Capo Testa (northern Sardinia, Italy). Facies, 56, 433-444.

Brandano M., Tomasetti L., Frezza V. (2015) – Halimeda dominance in the coastal wedge of Pietra di Finale (Ligurian Alps, Italy): The role of trophic conditions. Sedimentary Geology, 320, 30-37.

Brandano M., Cornacchia I., Raffi I., Tomassetti L. (2016) – The Oligocene–Miocene stratigraphic evolution of the Majella carbonate platform (Central Apennines, Italy) . Sedimentary Geology, 333, 1-14.

Brasier M.D. (1995a) – Fossil indicators of nutrient levels 1: eutrophication and climate change. In Bosence D.W.J., Allison P.A. (eds.): Marine Paleoenvironmental Analysis from Fossils. Geological Society Special Pubblication, 83, 113-132.

Brasier M.D. (1995b) – Fossil indicators of nutrient levels 2: evolution and extinction in relation to oligotrophy. In Bosence D.W.J., Allison P.A. (eds.): Marine Paleoenvironmental Analysis from Fossils. Geological Society Special Pubblication, 83, 133-150.

Cabadas H.V., Solleiro E., Sedov S., Pi T., Alcalà J.R. (2010) – The complex genesis of red soil in Penisula de Yucatan Mexico: mineralogical, micromorphological and geochemical proxies. Eurasian Soil Science, 43, 1439-1457.

Carannante G., Esteban M., Milliman J.D., Simone L. (1988) – Carbonate lithofacies as paleolatitude indicators: problems and limitations. Sedimentary Geology, 60, 333-346.

Coletti G., Basso D., Frixa A., Corselli C. (2015) – Transported rhodoliths witness the lost carbonate factory: a case history from the Miocene Pietra da Cantoni limestone (NW Italy). Rivista Italiana di Paleontologia e Stratigrafia, 121, 345-368.

Coletti G., Vezzoli G., Di Capua A., Basso D. (2016) – Reconstruction of a lost carbonate factory based on its biogenic detritus (Ternate-Travedona Formation and Gonfolite Lombarda Group - Northern Italy). Rivista Italiana di Paleontologia e Stratigrafia (in press).

Clari P., Dela Pierre F., Novaretti A., Timpanelli M. (1995) – Late Oligocen-Miocene sedimentary evolution of the critcal Alps-Apennines junction: the Monferrato area, Northwestern Italy. Terra Nova, 7, 144-152.

Cunningham K.J., Collins L.S. (2002) – Controls on facies and sequence stratigraphy of an upper Miocene carbonate ramp and platform, Melilla basin, NE Morocco. Sedimentary Geology, 146, 285-304.

D'Atri A., Dela Pierre F., Lanza, R., Ruffini R. (1999) – Distinguishing primary and resedimented vitric volcanoclastic layers in the Burdigalian carbonate shelf deposits in Monferrato (NW Italy). Sedimentary Geology, 129, 143-163.

D'Atri A., Dela Pierre F., Novaretti A., Cosca M.A., Hunziker J.C. (2001) – Miocene plankton biostratigraphy and $^{40}Ar/^{39}Ar$ dating. Eclogae Geolicae Helvetiae, 94, 137-144.

Demarcq G. (1970) – Etude stratigraphique du Miocène rhodanien. Mémoires du BRGM, 61, 257 pp.

Dercourt J., Gaetani M., Vrielynk B., Barrier E., Biju-Duval B., Brunet M.F., Cadet J.P, Crasquin S., Sandulescu M. (eds.) (2000) – Atlas Peri-Tethys, Palaeogeographical maps, 279 pp.

Espitalié J., Deroo G., Marquis F. (1985) – La Pyrolyse Rock-Eval et ses applications. Revue de l'Institut Français du Pétrole, 40, 563-579 and 755-784.

Flügel E. (2010) – Microfacies of Carbonate Rocks: Analysis Interpretation and Application. 1007 pp.

Föllmi K.B. (2016) – Sedimentary condensation. Earth-Sciences Reviews, 152, 143-180.

Fravega P., Piazza M., Vannucci G. (1989) – Archaeolithothamnium Rothpletz, indicatore ecologico-stratigrafico?. Simposio di Ecologia e Paleoecologia delle Comunità Bentoniche, Atti, 3, 729-743.

Geel T. (2000) – Recognition of the stratigraphic sequences in carbonate platform and slope deposits: empirical models based on microfacies analysis f Paleogene deposits in Southeastern Spain. Palaeogeography Palaeoclimatology Palaeoecology, 155, 211-238.

Grasso M., Pedley H.M. (1988) – The sedimentology and development of Terravecchia Formation carbonates (Upper Miocene) of North Central Sicily: Possible eustatic influence on facies development. Sedimentary Geology, 57, 131-149.

Gualtieri, A.F. (2000) – Accuracy of XRPD QPA using the combined Rietveld–RIR method. Journal of Applied Crystallography, 33, 267–278.

Guidry M.W., Mackenzie F.T. (2003) – Experimental study of igneous and sedimentary apatite dissolution: control of pH, distance from equilibrium, and temperature on dissolution rates. Geochimica et Cosmochimica Acta, 67, 2949-2963.

Hageman S.J., Lukasik J., McGowran B., Bone Y. (2003) – Paleoenvironmental significance of *Celleporaria* (Bryozoa) from modern and tertiary cool-water carbonates of Southern Australia. Palaios, 18, 510-527.

Halfar J., Godinez-Orta L., Mutti M., Valdez-Holguìn J.E., Borges J.M. (2004) – Nutrient and temperature controls on modern carbonate production: an example from the Gulf of California, Mexico. Geology, 32, 213-216.

Halfar J., Godinez-Orta L., Mutti M., Valdez-Holguìn J.E., Borges J.M. (2006) – Carbonates calibrated against oceanographic parameters along a latitudinal transect in the Gulf of California, Mexico. Sedimentology, 53, 297-320.

Halfar J., Eisele M., Riegl B., Hetzinger S., Godinez-Orta L. (2012) – Modern rhodolith-dominated carbonates at Punta Chivato Mexico. Geodiversitas 34, 99-113.

Hallock P., Schlager W. (1986) – Nutrient excess and the demise of coral reefs and carbonate platforms. Palaios, 1, 389-398.

Hallock P. (1988) – The role of nutrient availability in bioerosion: consequences to carbonate buildups. Palaeogeography, Palaeoclimatology, Palaeoecology, 63, 275-291.

Hallock P., Muller K.F.E., Halas J.C. (1993) – Coral reef decline - anthropogenic nutrients and the degradation of western Atlantic and Caribbean coral reefs. Research and Exploration, 9, 358-378.

Hallock P. (2001) – Coral reefs in the 21st century: is the past the key to the future? In Greenstein B.J., Carney C.K. (eds.): Proceedings of the 10th Symposium on the geology of the Bahamas and other carbonate regions. Gerace Research Center, San Salvador, Bahamas, 8-13.

Hallock P. (2005) - Global change and modern reefs: new opportunities to understand shallow-water carbonate depositional processes. Sedimentary Geology, 175, 19-33.

Holmes N.J., Harriot V.J., Banks S.A. (1997) – Latitudinal variation in patterns of colonisation of cryptic calcareous marine organisms. Marine Ecology Progress Series, 155, 103-113.

James N.P. (1997) - The cool-water carbonate depositional realm. In James N.P., Clarke J.A.D. (eds): Cool-Water Carbonates. SEPM Special Publication, 56, 1-22.

Jaquat O., Voegelin A., Juillot F., Kretzaschmar R. (2009) – Changes in Zn speciation during soil formation from Zn-rich limestones. Geochimica et Cosmochimica Acta, 73, 5554-5571.

Jessen C., Voolstra C.R., Wild C. (2014) – In situ effects of simulated overfishing and eutrophication on settlement of benthic coral reef invertebrates in the Central Red Sea . PeerJ 2:e339, DOI 10.7717/peerj.339.

Katz B.J. (1983) – Limitations of Rock-Eval pyrolysis for typing organic matter. Organic Geochemistry, 4, 195-199.

Klicpera A., Taylor P.D., Westphal H. (2013) – Bryoliths constructed by bryozoans in symbiotic associations with hermit crab in a tropical heterozoan carbonate system, Golfe d'Arguin, Mauritania. Marine Biodiversity, 43, 429-444.

Krom M.D., Berner R.A. (1981) – The diagenesis of phosphorus in near-shore marine sediments. Geochimica et Cosmochimica Acta, 45, 207-216.

Kühn V.O. (1963) – Korallensteinkerne im österreichischen Miozän. Annalen des Naturhistorischen Museums in Wien, 66, 101-112.

Langer M.R., Hottinger L. (2000) – Biogeography of selected "larger" foraminifera. Micropaleontology, 46, 105-126.

Langford F.F., Blanc-Valleron M.M. (1990) – Interpreting Rock-Eval pyrolysis data using graphs of pyrolizable hydrocarbon vs. total organic carbon. The American Association of Petroleum Geologist Bullettin, 74, 799-804.

Larson, A.C., and Von Dreele, R.B. (1999) – Generalized structure analysis system. Los Alamos National Lab, New Mexico, LAUR 86-748.

Lees A., Buller A.T. (1972) – Modern temperate-water and warm-water shelf carbonate sediments contrasted. Marine Geology, 13, 67-73.

Le Gall L., Payri C., Bittner L., Saunders G.W. (2009) – Multigene polygenetic analyses support recognition of the Sporolithales, ord. nov. Molecular Phylogenetics and Evolution, 54, 302-305.

Ma J.L., Wei G.J., Xu Y.G., Long W.G., Sun W.D. (2007) – Mobilizan and re-distribution of major and trace elements during extreme weathering of basalt in Hainan Island, South China . Geochimica et Cosmochimica Acta, 71, 3223–3237.

Maffione M., Speranza F., Faccenna C., Cascella A., Vignaroli G., Sagnotti L. (2008) – A synchronous Alpine and Corsica rotation. Journal of Geophysical Research, 113, doi:10.1029/2007JB005214.

Marinoni N., Pavese A., Riva A., Cella F., Cerulli T. (2007) – Chromatic weathering of black limestones quarried in Varenna (Lake Como, Italy). Building and Environment, 42, 68-77.

Mosbrugger M., Uterscher T., Dilcher D.L. (2005) – Cenozoic continental climatic evolution of Central Europe. Proceedings of the Natural Academy of Sciences U.S.A., 102, 14964-14969.

Mutti M., Hallock P. (2003) – Carbonate systems along nutrient and temperature gradient: some sedimentological and geochemical constraints. International Journal of Earth Sciences, 99, 833-849.

Nelson W.A., Sutherland J.E., Farr T.J., Hart D.R., Neill K.F., Kim H.J., Yoon H.S. (2015) – Multi-gene phylogenetic analyses of New Zealand coralline algae *Corallinapetra novaezelandiae* gen. et sp. nov. and recognition of the Hapalidiales ord. nov. Journal of Phycology, 51, 454-468.

Novaretti A., Bicchi E., Condello A., Ferrero E., Maia F., Tonon M., Torta D. (1995) – La successione oligo-miocenica del Monferrato: sintesi dei dati biostratigrafici. Atti del Convegno "Rapporti tra Alpi e Appennino" Peveragno (CN), Accademia Nazionale delle Scienze, Collana Scritti e Documenti, XIV, 39-59.

Nuñez-Betelu L., Baceta J.I. (1994) – Basics and applications of Rock-Eval/TOC pyrolysis: an example from the uppermost Paleocene/Lowermost Eocene in the Basque Basin, Western Pyreenes. Munibe, Ciencias Naturales, 46, 43-62.

Perrin C., Bosellini F. (2012) – Paleobiogeography of scleractinian reef corals: Changing patterns during the Oligocene–Miocene climatic transition in the Mediterranean. Earth Science Review, 111, 1-24.

Pomar L., Brandano M., Westphal H. (2004) – Environmental factors influencing skeletal grain sediment associations: a critical review of Miocene examples from the western Mediterranean. Sedimentology, 51, 627-651.

Pomar L., Hallock P. (2007) – Changes in coral-reef structure through the Miocene in the Mediterranean province: Adaptive versus environmental influence. Geology, 35, 899-902.

Pomar L., Hallock P. (2008) – Carbonate factories: A conundrum in sedimentary geology. Earth Sciences Reviews, 87, 134-169.

Renema W., Troelstra S.R. (2001) – Larger foraminifera distribution on a mesotrophic carbonate shelf in SW Sulawesi (Indonesia). Palaeogeography Palaeoclimatology Palaeoecology, 175, 125-146.

Reymond C.E., Zihrul K.S., Halfar J., Riegl B., Humphreys A., Westphal H. (2016) – Heterozoan carbonates from the equatorial rocky reefs of the Galápagos Archipelago. Sedimentology, 63, 940-958.

Reynaud J.Y., Dalrymple R.W., Vennin E., Parize O., Besson D., Rubino J.P. (2006) – Topographic controls on production and deposition of tidal cool-water carbonates, Uzès Basin, SE France. Journal of Sedimentary Research, 76, 116-129.

Reynaud J.Y., James N.P. (2012) – The Miocene Sommières basim. SE France: bioclastic carbonates in a tide dominated depositional system. Sedimentary Geology, 282, 360-373.

Rietveld, H.M. (1969) – A profile refinement method for nuclear and magnetic structures. Journal of Applied Crystallography, 2, 65–71.

Rösler A., Perfectti F., Peña V. & Braga J. C. (2016) – Phylogenetic relationships of corallinaceae (Corallinales, Rhodophyta): taxonomic implications for reef-building corallines. Journal of Phycology, doi: 10.1111/jpy.12404.

Ruffini R. (1995) – Evidenze di attività vulcanica terziaria nelle Alpi occidentali: problemi ed ipotesi. [PhD thesis]. 160 pp.

Ruttenberg K.C. (1992) – Development of a sequential extraction method for different form of phosphorus in marine sediments. Limnology and Oceanography, 37, 1460-1482.

Ruttenberg K.C., Berner R.A. (1993) – Authigenic apatite formation and burial in sediments from non-upwelling, continental margin environments. Geochimica et Cosmochimica Acta, 57, 991-1007.

Ruttenberg K.C. (2004) The global phosphorus cycle. In Holland H.D., Turekian K.K. (eds.): Treatise on Geochemistry. Vol. 8, 585-643.

Ruttenberg K.C., Ogawa N.O., Tamburini F., Briggs R.A., Colasacco N.D., Joyce E. (2009) – Improved, high throughput approach for phosphorus speciation in natural sediments via the SEDEX sequential extraction method. Limnology and Oceanography: Methods, 7, 319-333.

Schüttenhelm R.T.E. (1976) – History and modes of Miocene carbonate deposition in the interior of the Piedmont Basin, NW Italy. [PhD thesis]. Utrecth Micropaleontological Bull, 4, 207 pp.

Slomp C.P., Thomson J., deLange G.J. (2002) – Enhanced regeneration of phosphorus during formation of the most recent eastern Mediterranean sapropel (S1). Geochimica et Cosmochimica Acta, 66, 1171-1184.

Stalder C., Spezzaferri S., Rüggeberg A., Pirkenseer C., Gennari G. (2014) – Late Weichselian deglaciation and early Holocene development of a cold-water coral reef along the Lopphavet shelf (Northern Norway) recorded by benthic foraminifera and ostracoda
. Deep-Sea Research II, 249-269.

Toby, B.H. (2001) – EXPGUI, a graphical user interface for GSAS. Journal of Applied Crystallography, 34, 210–213.

Tyrrell T. (1999) – The relative influence of nitrogen and phosphorus on ocean primary production. Nature, 400, 525-531.

Vannucci G., Piazza M., Fravega P., Abate C. (1996) – Litostratigrafia e paleoecologia di successioni a rodoliti della Pietra da Cantoni (Monferrato Orientale, Italia Nord-Occidentale). Atti della Società Toscana di Scienze Naturali, Memorie, Seria A, 103, 69-86.

Vannucci G., Quaranta F., Piazza M., Fravega P. (2003) - The Oligocene reefal facies of Bric San Bernardino (Millesimo, NW Italy). Le facies recifali oligoceniche di Bric San Bernardino (Millesimo, Italia nord-occidentale). Atti Ticinesi di Scienze della Terra, 44, 35-44.

Wade B.S., Pearson P.N., Berggren W.A., Pälike H. (2011) – Review and revision of Cenozoic tropical planktonic foraminiferal biostratigraphy and calibration to the geomagnetic polarity and astronomical time scale. Earth-Science Review, 104, 111-142.

Wilson M.E.J., Vecsei A. (2005) – The apparent paradox of abundant foramol facies in low latitudes: their environmental significance and effect on platform development . Earth-Science Reviews, 69, 133-168.

Wood R. (1993) – Nutrients, Predation and the History of Reef-Building. Palaios 8, 526-543.

Zachos J., Pagani M., Sloan L., Thomas E., Billups K. (2001) – Trends, Rhythms, and Aberrations in Global Climate 65 Ma to Present. Science, 292, 686-693.

Figure Caption

Figure 1: Location of the studied outcrops in the European A) and regional B) context. C) Location of the outcrop of Uviglie (45°4.70' N; 8° 24.79' E) in the Piedmont Basin. D) Location of the outcrops of Souvignargues (43° 48.39' N; 4° 7.15' E) and Pondres (43° 48.46' N; 4° 5.94' E) in the Sommières Basin.

Figure 2: Stratigraphic framework of the studied units. The stratigraphic framework, the environmental interpretation of the Sommières Basin, and the approximate stratigraphic position of the Sandy Molasse Unit are based on Berger (1974) and Reynaud & James (2012); the stratigraphic log of the basin is modified from Reynaud & James (2012). The stratigraphic framework and the environmental interpretation of Sequence of PDC are based on Novaretti et al. (1995), Ruffini (1995), D'Atri et al. (1999, 2001) and Coletti et al. (2015). The two logs have different scale.

Figure 3: Succession of Uviglie. A) Rhodolith floatstone; lithozone UV2, Lower Unit. B) Bed of condensed sediments at the base of the Upper Unit; lithozone UV5. C) Encrusting coralline alga of the Hapalidiales order. D) Coralline alga, of the Hapalidiales order, growing around a plate of a barnacle shell. E) Fragment of a barnacle plate. F) large benthic foraminifera of the lepidocyclinid group.

Figure 4: Simplified log of the studied successions. The first column include the Dunham classification of the lithozones; mds = mudstone; wck = wackestone; pck = packstone; grn = grainstone; flt = floatstone; rds = rudstone. The scale bar on the side of the log is 1 m long. The key to symbols of the skeletal grains is the same of Figure 2. The second, third, fourth and fifth column include compositional data; the data of the different variables of each column are overlapped and not stacked.

Figure 5: Sandy Molasse Unit of the Sommières Basin. A) Bryozoans nodules; Pondres. B) Bryozoans dominated grainstone; lithozone PON3. C) Rhodoliths = r; lithozone PON4. D) Branch of a coralline alga of the Hapalidiales order; lithozone PON4. E) Encrusting coralline alga of the Hapalidiales order; lithozone PON1. F) *Amphistegina*; lithozone PON4.

Figure 6: Authigenic minerals. A) Mature glaucony grains; Upper Unit, Pietra da Cantoni. B) Planktonic foraminifera packstone with common grains of authigenic minerals; Upper Unit Pietra da Cantoni. C) Authigenic phosphate mineral replacing biogenic calcite; lithozone SOUV1, Sommières Basin; point G = EDS analysis included in panel G. D) Immature glaucony filling the chambers of a benthic foraminifer; lithozone PON3, Sommières Basin; gl = glaucony. E) Echinoid spine with authigenic phosphate replacing calcite; lithozone PON2, Sommières Basin. F) The same echinoid spine of panel E, observed with backscatter electrons that highlight the difference in composition between the calcite and the replacing phosphate; point H = EDS analysis included in panel H. G) EDS spectrum of point G of panel C; x-axis = energy (kilo-electronvolt); y-axis = counts (kilo-counts). H) EDS spectrum of point H of panel F; ; x-axis = energy (kilo-electronvolt); y-axis = counts (kilo-counts).

Figure 7: Paleoenvironmental reconstruction; the key for the symbols used in this figure is included in Figure 2. A) Model of the PDC basin during the deposition of the Lower Unit; arrow = source of phosphates; the size of bioclast symbols is unrelated to their abundance B) Model of the Sommières Basin during the deposition of the Sandy Molasse Unit; arrows =source of phosphates; the size of bioclast symbols is unrelated to their abundance. C) Distribution of the different carbonate factories, symbolized by the dominant carbonate producers, in the Gulf of California (Halfar et al., 2004), plotted against chlorophyllα concentration (GIOVANNI, NASA, Acker and Leptoukh, 2007). D)

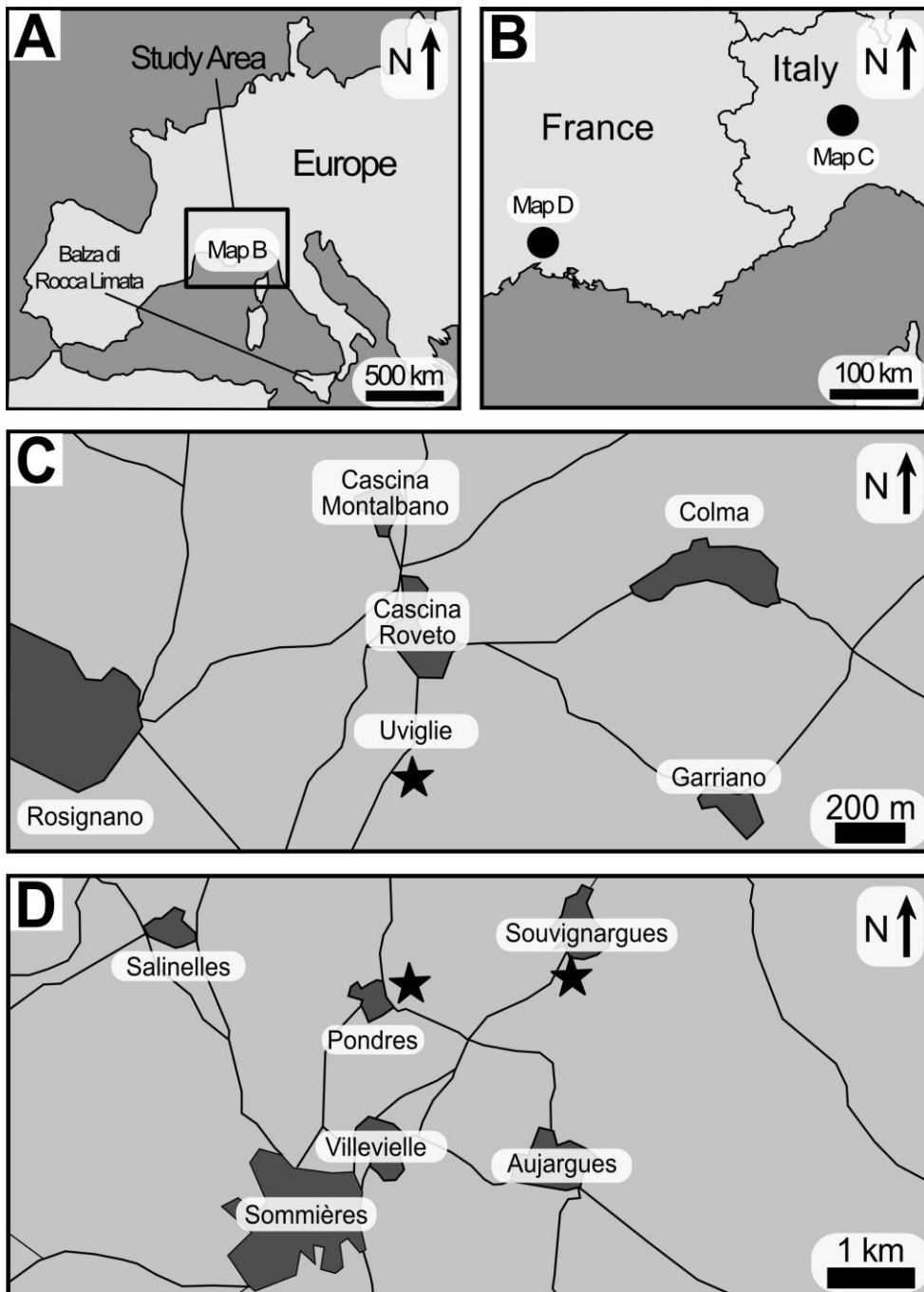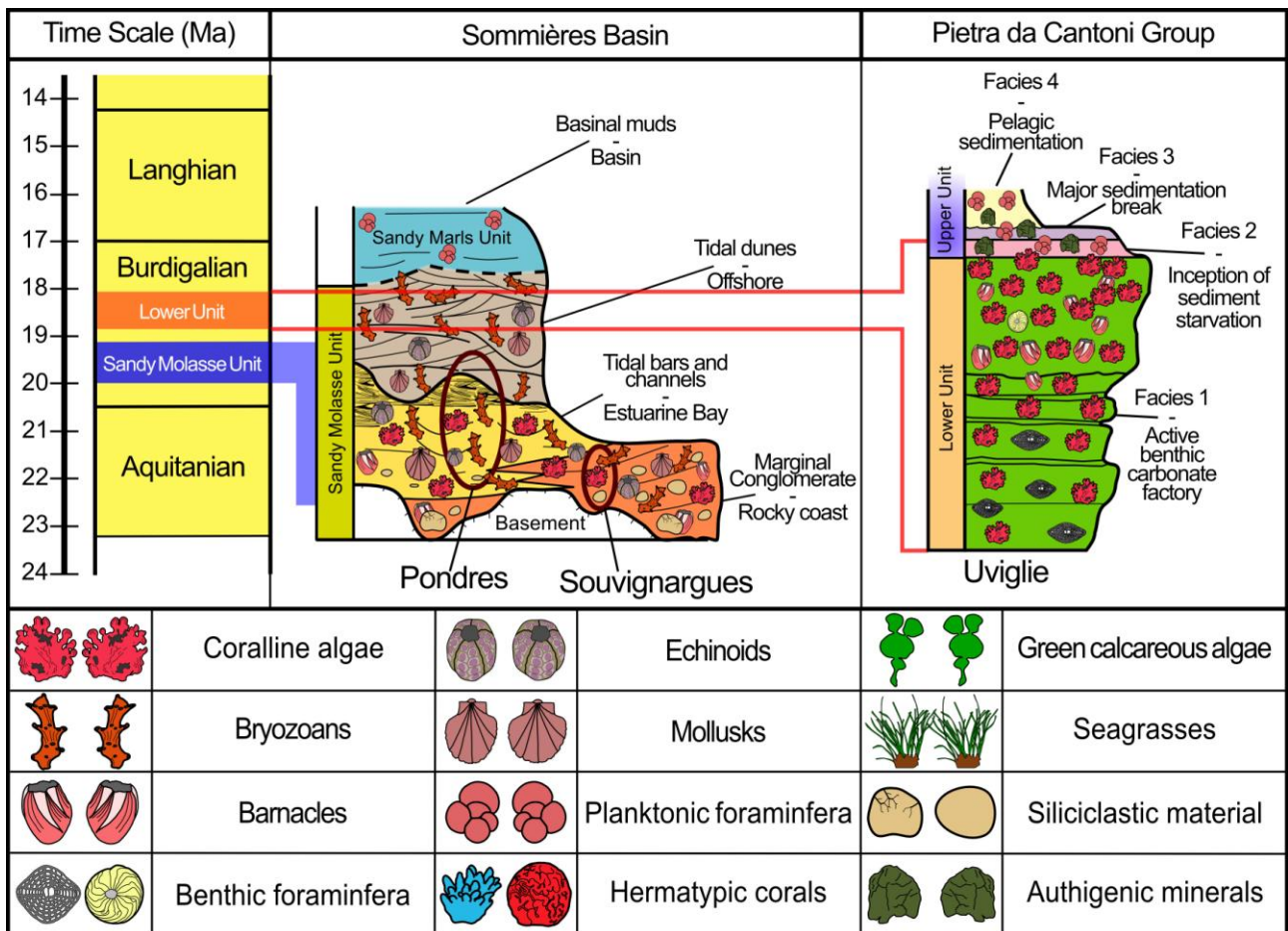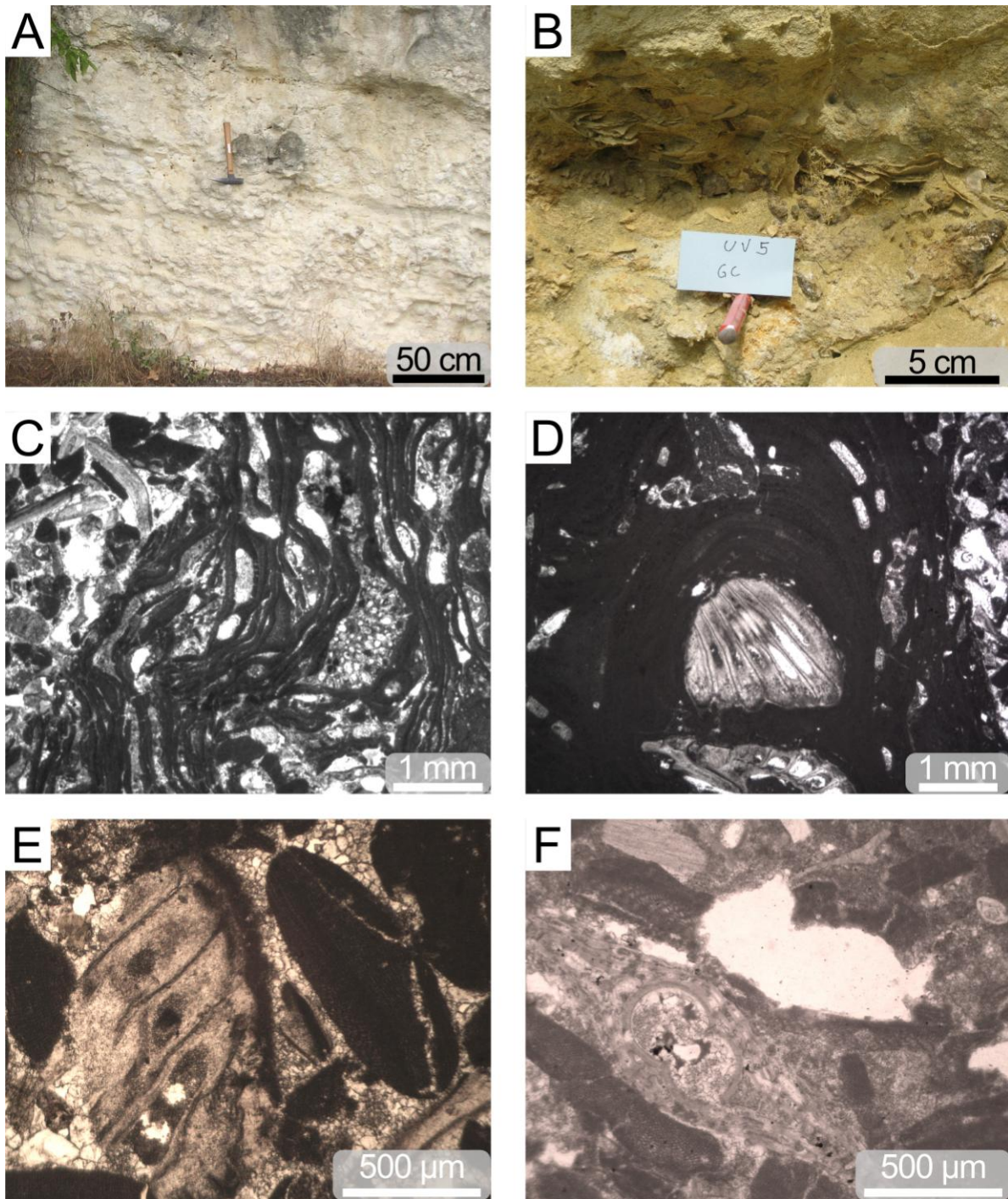General schematic, nutrient-based, distribution of benthic carbonate factories in the Mediterranean basin, during the Miocene.
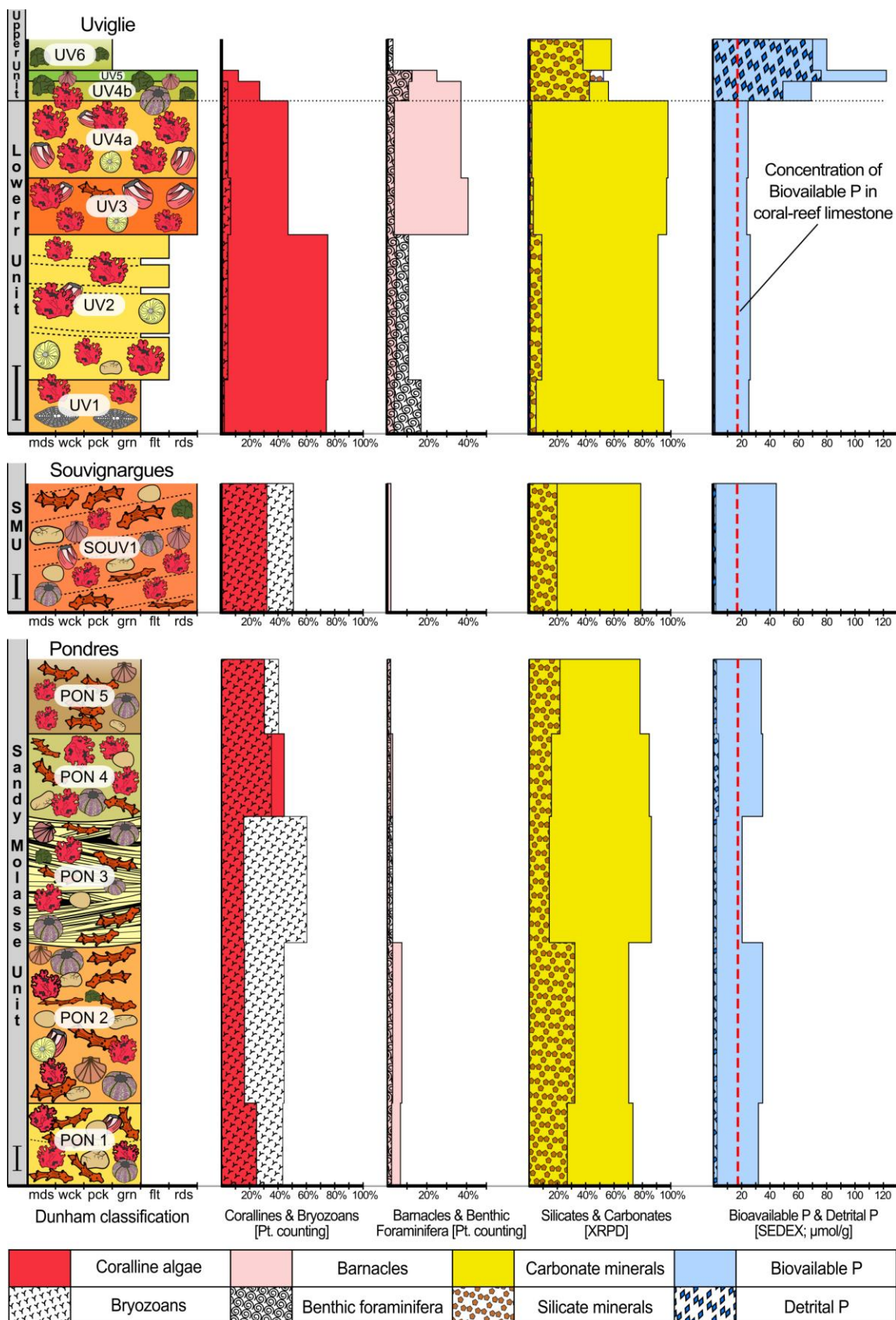
Fig. 1

Fig. 2

Fig. 3

Fig. 4
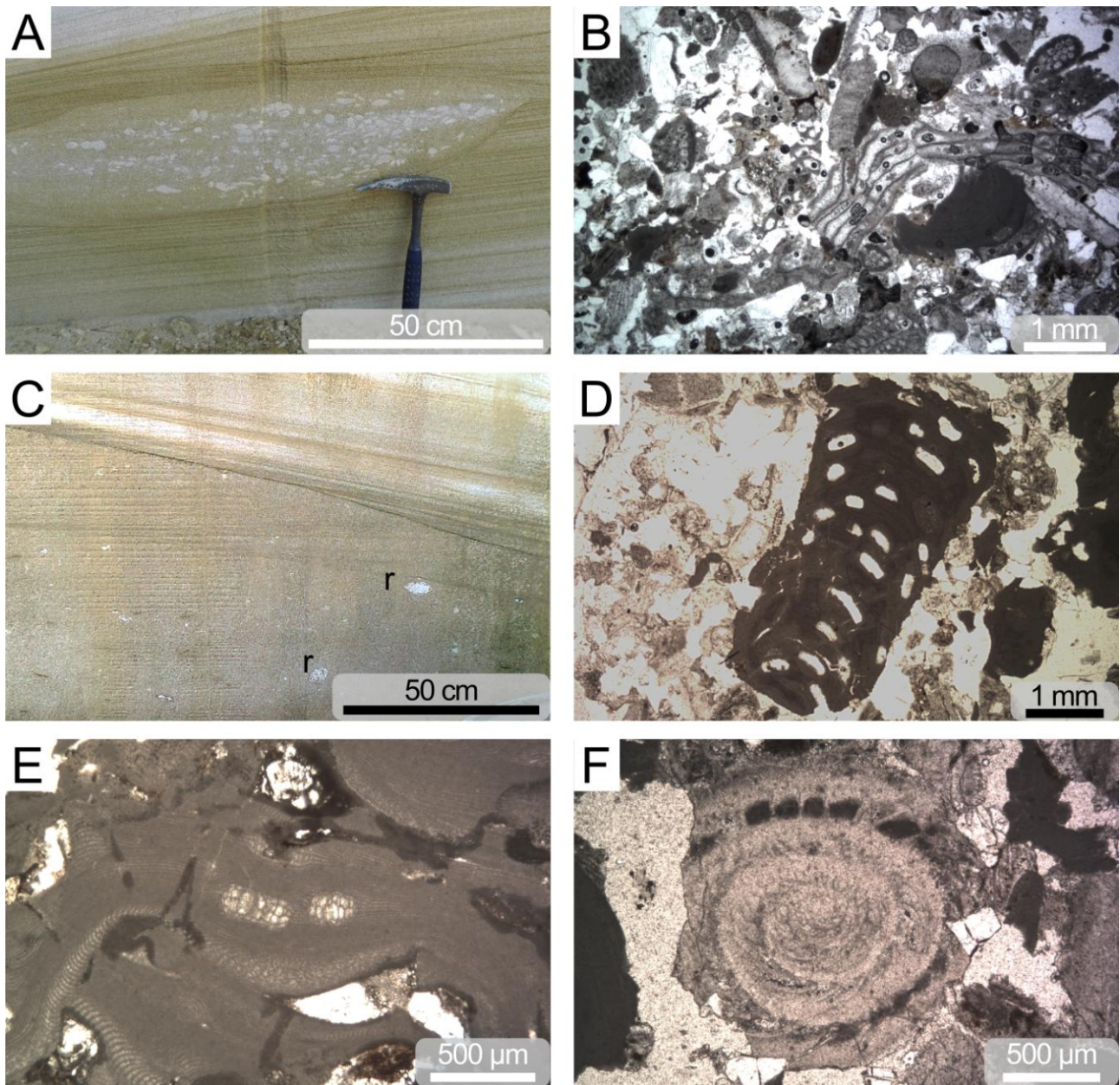
Fig. 5
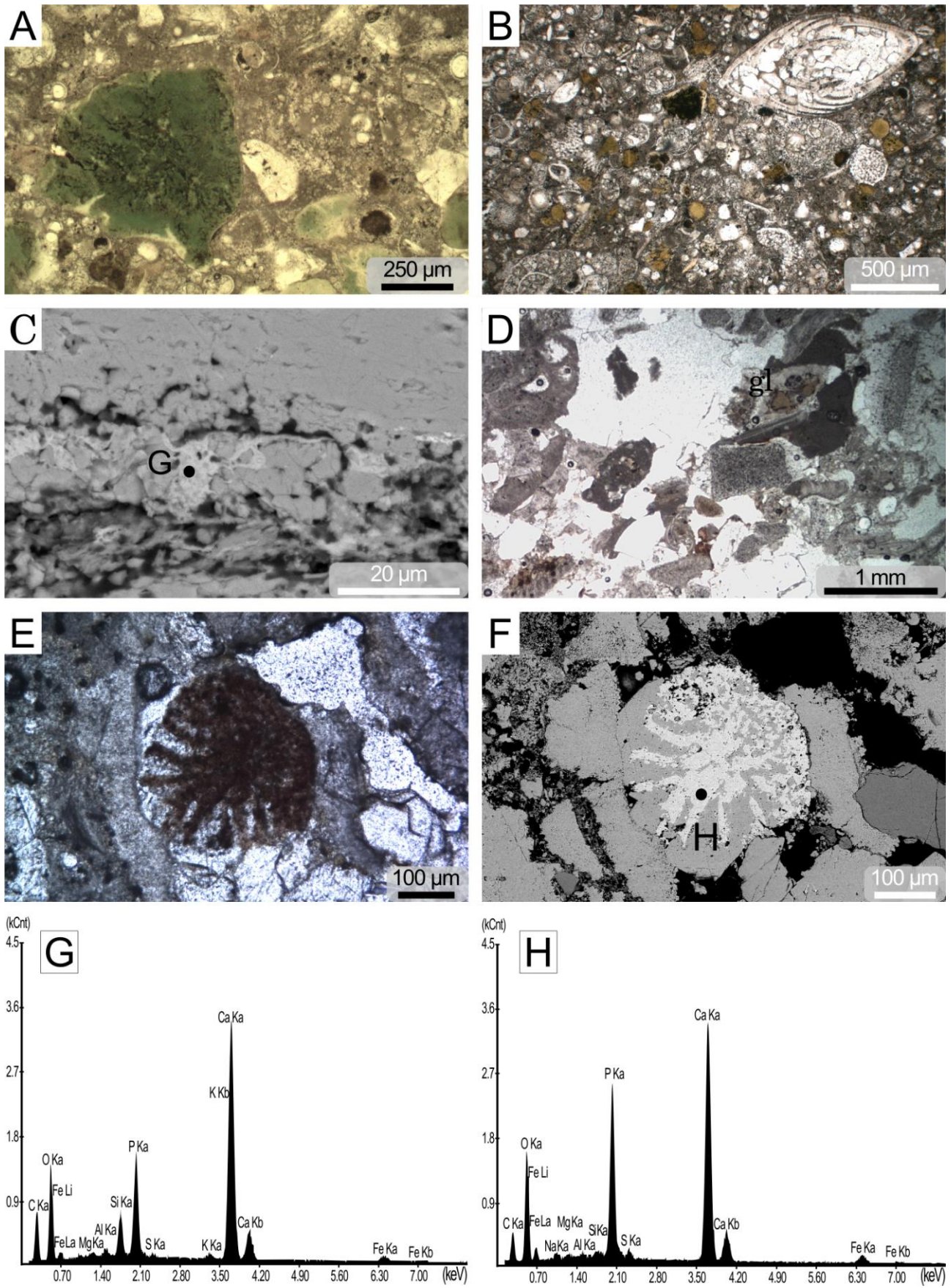
Fig. 6
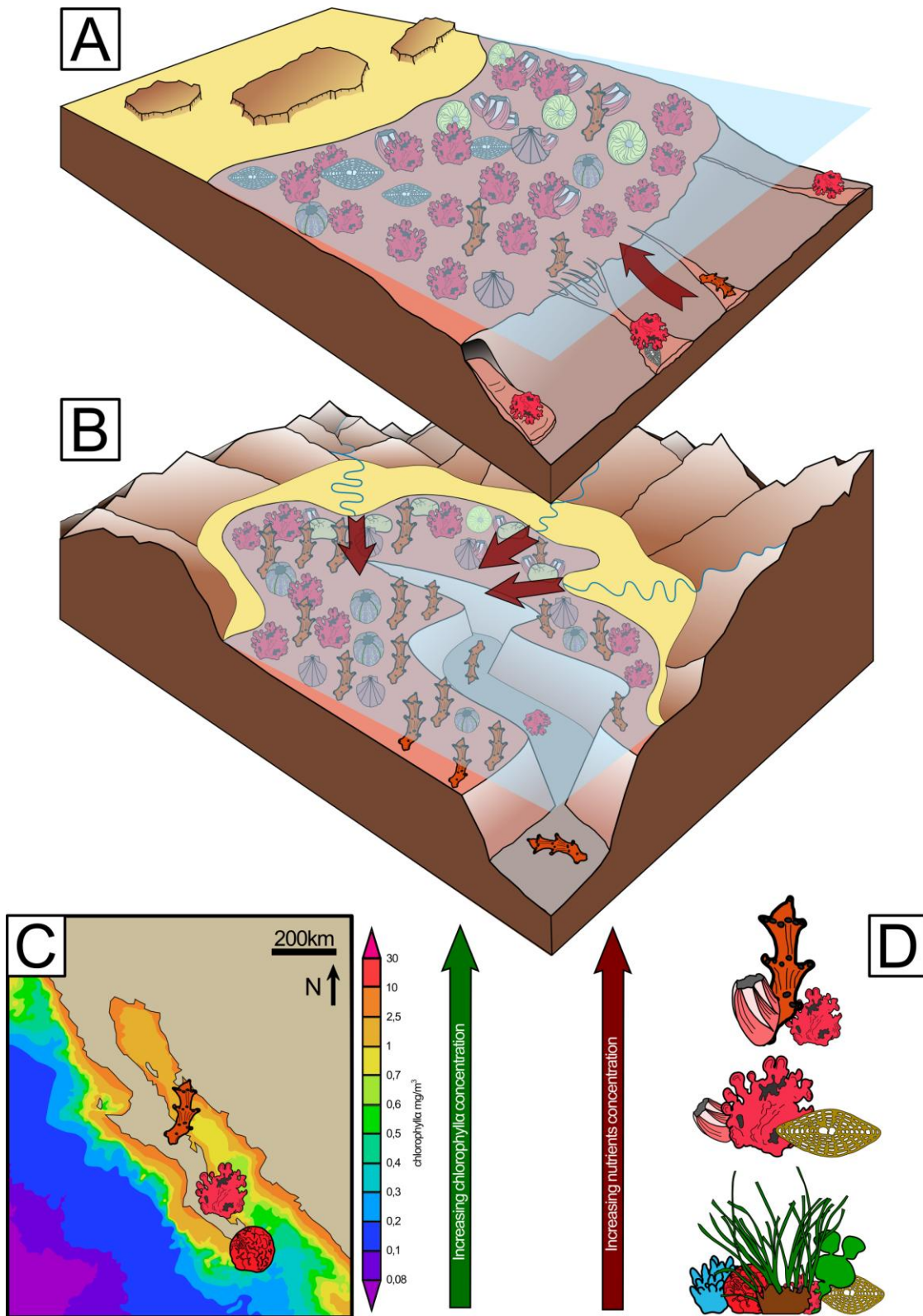
Fig. 7

Table caption

Table 1: Summary of the data of the lithozones of the studied succession.

Table 1

Skeletal assemblage	Lithozones [Point counting]													Balza di Rocca Limata
	UV1	UV2	UV3	UV4a	UV4b	UV5	UV6	PON1	PON2	PON3	PON4	PON5	SOUV1	
Coralline algae	74%	75.1%	47%	47.1%	27.4%	12.8%	0%	24.7%	16.1%	15.7%	43.7%	30%	32.4%	Hermatypic corals
Bryozoans	2.3%	4.6%	6.4%	4.5%	4.7%	0%	0%	43.2%	44.3%	56.6%	35.2%	40%	51%	
Barnacles	3.6%	4.4%	41.4%	37.7%	25%	0%	0%	6.2%	6.5%	1%	2.3%	1.4%	2%	
Benthic foraminifera	17%	10.7%	3.4%	3.7%	10.8%	12.5%	2.9%	1.8%	2.6%	2.2%	1.5%	1.8%	0.1%	
Planktonic foraminifera	0%	0.2%	0%	0.6%	17.5%	66.4%	97%	0%	0%	0%	0%	0%	0%	
Echinoids	1.8%	2.5%	1%	2.2%	5.6%	0%	0%	19.1%	23.2%	19.1%	10.2%	14.4%	5%	
Mollusks	0.3%	1.9%	0.7%	3.1%	7.1%	8.3%	0%	4.8%	6.5%	5.2%	7%	11.9%	9.5%	
Brachiopods	0%	0%	0%	0%	0%	0%	0%	0.2%	0.8%	0.2%	0.1%<	0.4%	0%	
Ostracods	0%	0.1%	0%	0.6%	1.4%	0%	0.1%	0.1%<	0%	0%	0.1%<	0%	0%	
Serpulids	1%	0.5%	0.1%	0.5%	0.5%	0%	0%	0%	0%	0%	0%	0.1%	0%	
Coralline-algal abundance [Digital mapping]														
Hapalidiales	99.7%	98.6%	98.2%	83.2%				92.8%		99.5%	95.2%	100%	85%	
Corallinales	0.3%	1.4%	0.8%	8.6%				7.2%		0.5%	4.8%	0%	9.5%	
Sporolithales	0%	0%	1,00%	8.2%				0%		0%	0%	0%	5.5%	
Phosphorus content (µmol P /g of sample)														
Bioavailable P	25.38	26.2	23.62	24.48	69.01	121.95	83.39	31.64	34.51	24.2	34.31	33.71	44.44	16.78
Detrital P	0.37	0.98	0.48	0.76	48.76	75.76	70.22	2.15	2.15	1.83	3.27	2.13	2.03	0.89
Detrital and authigenic fractions [Point counting]														
Detrital fraction	0.4%	1.6%	0.5%	2.1%	10.7%	19.5%	10.6%	33.5%	38.7%	22.7%	22%	26%	30.8%	1.8%
Bioclastic fragments	99.5%	98.3%	99.5%	97.8%	75.3%	46.4%	68.2%	66.4%	61.2%	77.3%	78%	75.9%	69.2%	98.2%
Authigenic minerals	Traces	Traces	Traces	Traces	14%	34.1%	21.2%	Traces	Traces	Traces	Traces	Traces	Traces	0%
Quantitative X-ray powder diffraction														
Silicate minerals	4.9%	8.9%	2.3%	2%	42.5%	52.6%	37.8%	26.7%	32%	13.8%	15.4%	21.6%	20.4%	6%
Carbonate minerals	95.1%	91.1%	97.3%	97.7%	55.8%	43.5%	57.8%	73.3%	67.9%	86.2%	84.5%	78.3%	79.2%	94%
Carbonate-Apatite	Traces	Traces	Traces	Traces	1.4%	3.7%	4.4%	Traces	Traces	Traces	Traces	Traces	Traces	Traces

Highlights

Integrated analyses of two coeval Miocene limestones are performed
The results support the use of SEDEX extraction for the study of palaeo-nutrient levels
Nutrient-based distribution of Miocene carbonates mimics the one of modern oceans